Journal of Neural Engineering

PAPER

Cortico-muscular functional network: an exploration of cortico-muscular coupling in hand movements

Journal of Neural Engineering

PAPER

Cortico-muscular functional network: an exploration of cortico-muscular coupling in hand movements

Xugang Xi[1,2,*], Xiangxiang Wu[1,2], Yun-Bo Zhao[3], Junhong Wang[1,2], Wanzeng Kong[2,4] and Zhizeng Luo[1,2]

[1] School of Automation, Hangzhou Dianzi University, Hangzhou 310018, People's Republic of China
[2] Key Laboratory of Brain Machine Collaborative Intelligence of Zhejiang Province, Hangzhou 310018, People's Republic of China
[3] Department of Automation, University of Science and Technology of China, Hefei, People's Republic of China
[4] School of Computer Science and Technology, Hangzhou Dianzi University, Hangzhou 310018, People's Republic of China
[*] Author to whom any correspondence should be addressed.

E-mail: xixi@hdu.edu.cn

RECEIVED
23 November 2020

REVISED
18 May 2021

ACCEPTED FOR PUBLICATION
26 May 2021

PUBLISHED
9 June 2021

Keywords: cortico-muscular functional network, coupling, electroencephalography, electromyography, transfer entropy

Abstract

Objective. The main objective of this research was to study cortico-muscular, intra-cortical, and inter-muscular coupling. Herein, we established a cortico-muscular functional network (CMFN) to assess the network differences associated with making a fist, opening the hand, and wrist flexion. *Approach*. We used transfer entropy (TE) to calculate the causality between electroencephalographic and electromyographic data and established the TE connection matrix. We then applied graph theory to analyze the clustering coefficient, global efficiency, and small-world attributes of the CMFN. We also used Relief-F to extract the features of the TE connection matrix of the beta2 band for the different hand movements and observed high accuracy when this feature was used for action recognition. *Main results*. We found that the CMFN of the three actions in the beta band had small-world attributes, among which the beta2 band's small-world was stronger. Moreover, we found that the extracted features were mainly concentrated in the left frontal area, left motor area, occipital lobe, and related muscles, suggesting that the CMFN could be used to assess the coupling differences between the cortex and the muscles that are associated with different hand movements. Overall, our results showed that the beta2 (21–35 Hz) wave is the main information carrier between the cortex and the muscles, and the CMFN can be used in the beta2 band to assess cortico-muscular coupling. *Significance*. Our study preliminarily explored the CMFN associated with hand movements, providing additional insights regarding the transmission of information between the cortex and the muscles, thereby laying a foundation for future rehabilitation therapy targeting pathological cortical areas in stroke patients.

1. Introduction

Establishing the distinct functional and structural relationship between the cortex and the musculature, in the context of movement, is a major goal of neurology. Electroencephalography (EEG) and electromyography (EMG) help define this relationship by recording the signals produced by cortical activity, and the signals produced by muscle group activity, respectively. During body movement, the motor cortex sends a command to the control limb; at the same time, the limb returns the signal to the cortex to produce the action. This relationship between the cortex and the muscles can be expressed as cortico-muscular coherence (CMC) [1] The CMC between EEG and EMG has been proposed to reflect a signal that the cortex is regaining muscle control. The cortico-muscular functional network (CMFN) can be used, as such, in the fields of rehabilitation prediction, rehabilitation therapy, and artificial limb support. Krauth *et al* [2] demonstrated that, in stroke patients, CMC can serve as a marker of motor recovery and can provide information on the specific cortical areas that respond to rehabilitation treatments based on real-time EEG. Artoni *et al* [3] showed that even under the condition of stationary treadmill walking, the human motor cortex could actively control the contralateral leg muscles. Lai *et al* [4] showed that the

CMC can detect the neuromuscular changes induced by peripheral electrical stimulation. Therefore, our research focused on the establishment and analysis of the CMFN to improve our understanding of this relationship.

Recently, cortico-muscular coupling analytical methods have made great progress. The main methods to establish functional coupling are the Pearson's correlation coefficient [5], spectral coherence [6], mutual information [7], phase locking value [8], and partial directed coherence [9, 10]. The coupling model between cortical muscles remains unknown, and the connection between EEG and EMG data has nonlinear causality. Therefore, the Pearson's correlation coefficient and spectral coherence cannot effectively describe the coupling characteristics between the cortex and the muscles. Transfer entropy (TE) does not require an established model or a nonlinear quantitative analysis and can hence estimate the directional strength of two-way coupling between the cortex and the muscles (downlink EEG $\rightarrow$ EMG and uplink EMG $\rightarrow$ EEG) [11]. Shovon [12] demonstrated the application of TE in the evaluation of directed functional brain networks. This study focused on TE values to assess the coupling between the cortex and the muscles. The TE connection matrix was filtered using the threshold method to remove false connections, and an effective connection matrix was obtained. Thereafter, the CMFN was established using the efficient connection matrix.

The cortex and the muscle groups form a complex system composed of hundreds of billions of neurons [13]. All movements are coordinated by multiple cortical regions and multiple muscles working together. Considering several muscle groups of the cortex and upper limbs as a whole, the application of the study of complex network theory [14] is very important for understanding the coupling relationship between the cortex and the muscle groups and for elucidating the behavioral relationship between them. For regular networks, the small-world networks in complex networks have smaller, shorter paths but possess larger clustering coefficients for random networks. In recent years, research on the prediction and diagnosis of brain diseases has garnered the attention of many scholars. Majnu [15] used a complex network to evaluate patients in the early stages of Alzheimer's disease and discovered that the volumetric network was affected in a non-global manner during the neurodegenerative process.

Currently, most scholars recognize hand movements by fusing information features [16]. In this study, we identified hand movements through the TE connection matrix. As a feature, we took the value of each connection of the connection matrix (25×25) for each action that passed the TE calculations, such that there were 600 ($25 \times (25 - 1)$) eigenvalues. Next, we extracted the relevant features from the 600, and deleted irrelevant features. We used the extracted features to recognize the hand movements and obtained high recognition accuracy. We also discovered that these feature edges were mainly concentrated in the connection between the left cortex area and its related muscles. These results demonstrate that the CMFN could be used to detect differences in the coupling between the cortex and the muscles for different hand movements.

2. Methods

2.1. Framework

We analyzed EEG and EMG data from six participants who performed three hand movement experiments. The establishment and analysis of the CMFN based on the recorded data included the following steps (shown as a schematic in figure 1): (a) EEG and EMG data were preprocessed and filtered into four frequency bands (theta: 4–8 Hz, alpha: 8–13 Hz, beta1: 13–21 Hz, and beta2: 21–35 Hz). (b) The TE connection matrix was obtained by calculating the causal relationship between the data by the TE. (c) The TE connection matrix was selected by the threshold (T), and the false connections between electrodes were removed, allowing construction of a directed connection network (connection matrix). (d) According to graph theoretical methods, it was shown that the CMFN has small-world attributes, after which the preliminary CMFN was established. (e) A ReliefF pair TE connection matrix was used to extract features for action recognition. (f) Training support vector machines (SVM) and logistic regression (LR) models were used for action recognition.

2.2. Participants and experimental design

Six healthy participants were recruited (four males and two females; age: 22 and 23 years). All participants provided signed informed consent according to the Helsinki Declaration, and all measurements were approved by the Hangzhou Dianzi University's Institutional Review Board. The participants, who had no history of mental illness participated in the study. The participants did not drink alcohol, coffee, strong tea, or sports drinks the day before the experiment nor did they smoke or exercise vigorously. Two hours before the experiment, the participants' hair was shampooed to remove cutin and their hair was blown dry. The laboratory consisted of a quiet shielded room, in which the air conditioning and lights were turned off to reduce the power frequency interference. Participants sat quietly in comfortable seats facing the screen and made a fist (MF), opened the hand (OH), and performed wrist flexion (WF) movements according to the instructions on the screen. The general experimental process is illustrated in figure 2 and includes the preparation and rest time (5 min), each action time (3 s) and the time between each action to rest and prepare for the subsequent action (1 min). Each subject performed the above

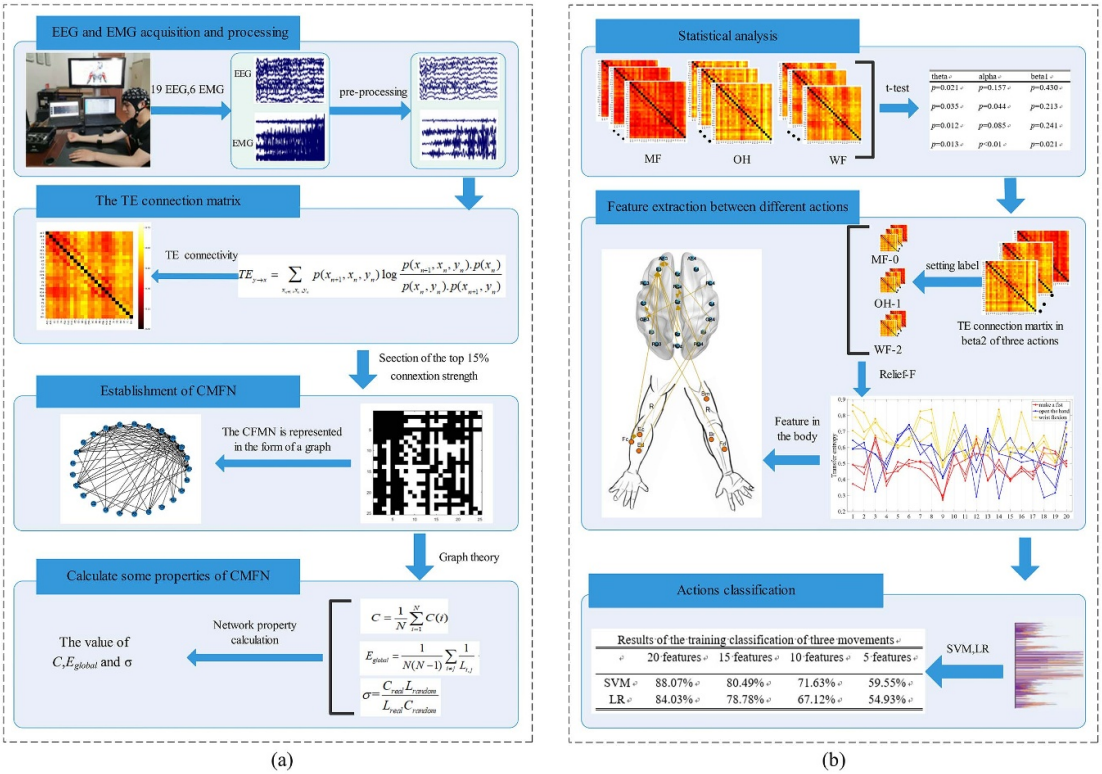

Figure 1. Establishment and analysis of the CMFN. (a) Establishment and calculation of CMFN. (b) Actions classification.

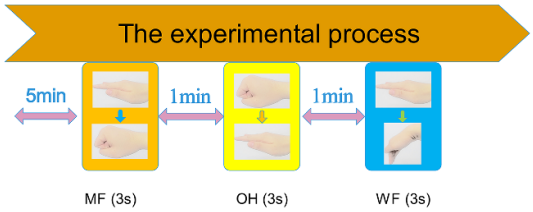

Figure 2. Experimental design. The time from start to end of each action is 3 s.

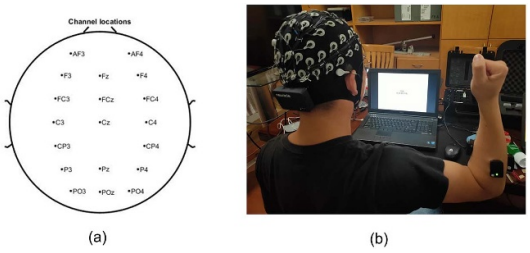

Figure 3. Experimental process. (a) EEG electrode arrangement. (b) Participants take corresponding actions according to the instructions on the screen.

experiment ten times, and the rest time between each experiment was 10 min.

In the experiments, a 64 channel wireless EEG amplifier (NeuSen.W64, Neuracle, China) was used, with a sampling frequency of 1000 Hz. Before data collection, the impedance was kept below 5 kΩ by injecting a conductive paste. The selected motor cortex electrodes are shown in figure 3(a), including 19 channels (motor cortex electrode: AF3, AF4, F3, FZ, F4, FC3, FCZ, FC4, C3, CZ, C4, CP3, CP4, P3, PZ, P4, PO3, POZ, and PO4) selected from 59 channels from the cortical EEG. Such electrode selection facilitates a thorough assessment of the motor cortex, and ensures that the signal interference between the electrodes remains small. EMG recordings were collected using the Trigno TM wireless EMG (DelsysInc, Natick, MA, USA) equipment with a sampling frequency of 1926 Hz. The EMG data were acquired at the brachioradialis (Br), flexor digitorum superficialis (Fd), extensor digitorum (Ed), extensor carpi ulnaris (Ec), flexor carpi ulnaris (Fc), and bicipital muscle of arm (Bm). The participants followed the instructions on a computer screen (figure 3(b)).

2.3. Pre-processing

The EEGLAB [17] toolbox was used to process the EEG data. To determine the average reference for the EEG data, the AAR [18] plugin was used for blind source separation of EEG data to remove EMG and electro-oculogram (EOG) ingredients. The ICA was used to remove other artifacts, after which the data were processed by bandpass filtered between 1 and 38 Hz (two-pass Butterworth filter at the third order) and finally downsampling to 250 Hz. In order to eliminate part of the somatosensory response contained in

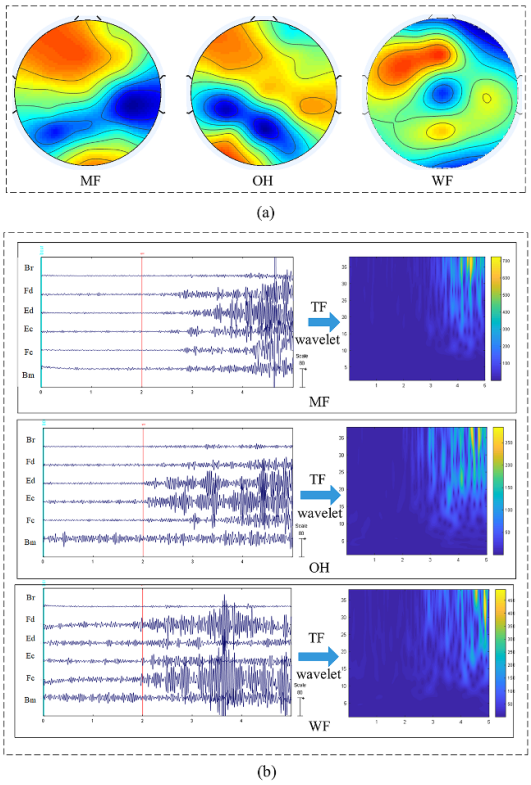

Figure 4. Analysis of EEG and EMG. (a) Averaged topographical map of brain of MF, OH and WF. (b) EMG response in both temporal and time- frequency domain of MF, OH and WF (movement started at 2 s).

the EEG, firstly, the average value between the waveforms of the left cortex area and the right cortex area was calculated. Secondly, the difference between the left cortex area and the right cortex area was calculated as a difference wave [19]. Finally, the difference wave was subtracted from the waveform in the left cortex area. The EMG data were first denoised by wavelet [20] and bandpass filtered between 1 and 38 Hz (two-pass Butterworth filter at the third order). The data were then processed by downsampling to 250 Hz. Finally, EEG and EMG data were matched according to the type of movement and time.

Wavelet analysis on the preprocessed EEG was performed, the energy of each lead found and rendered into an energy topographical map of the brain on a two-dimensional plane. As shown in the figure 4(a), topographical map of brain of average energy of MF, OH and WF movement (times: 0–3 s), EEG energy is mainly concentrated on the hemisphere of the left frontal lobe during MF, OH and WF actions. For the preprocessed EMG signal, first we superimpose and average the time domain information from 2 s before the start of the action to 3 s after. The wavelet function was then used to perform time-frequency (TF) [21] analysis of the EMG and average of all EMG time domain (figure 4(b)). It can be seen from the time-domain information that the larger amplitudes are Fd and Ed in MF, Ed and Ec in OH, and Fd and Fc in WF. It could be seen from the averaged TF maps that the changes in myoelectric energy in the 1–38 Hz channel were all caused by movement.

2.4. TE

The information of multiple time and space interactions of the EEG and EMG data can indicate the functional relationship between the cerebral cortex and muscle. TE is a non-parametric statistic measuring the amount of directed (time-asymmetric) transfer of information between two random processes. The TE from one process, denoted x, to another process, denoted y, represents the amount of uncertainty reduced by knowing the past value of x and the future value of y given the past value of y. For the autoregressive process, TE is reduced to Granger causality. Thus, when the model of Granger causality is not established, TE is very beneficial to analyze nonlinear signals (e.g. EEG, EMG, and EOG) [22].

TE estimates the amount of information passed to a time series that does not depend on its own past activities, but on the past activities of another time series. Given two processes x and y, the TE from y to x is computed as:

$$\mathrm{TE}_{y\to x} = \sum_{x_{n+1},x_n,y_n} p(x_{n+1},x_n,y_n) \times \log \frac{p(x_{n+1},x_n,y_n).p(x_n)}{p(x_n,y_n).p(x_{n+1},y_n)} \quad (1)$$

where, $p(x_{n+1}, x_n, y_n)$ is the transition probability.

2.5. Graph analysis

An $N \times N$ ($N = 25$, 19 EEG electrodes and six EMG electrodes) binary graph cortico-muscular functional coupling network, consisting of nodes (cortex and muscle components) and directed edges (connectivity) between the nodes, could be constructed by applying a threshold (T, top 15% connection strength) to the connection matrix calculated by TE.

The clustering coefficient [23] of node i in the graph refers to the ratio between the actual number of edges between all neighboring nodes connected with node i (excluding node i) and the number of edges with the maximum energy between these neighbor nodes. The clustering coefficient $C(i)$ is defined as:

$$C(i) = \frac{2E_i}{K_i(K_i-1)}. \quad (2)$$

For the whole network, the value of the clustering coefficient (C) is equal to the average value of each node $C(i)$:

$$C = \frac{1}{N}\sum_{i=1}^{N} C(i). \quad (3)$$

The characteristic path length (L) of the network is the average of the shortest path length between all node pairs:

$$L = \frac{1}{N(N-1)} \sum_{i \neq j} l_{ij}. \quad (4)$$

The global efficiency (E_{global}) is the mean of the reciprocal of the shortest path length between all node pairs:

$$E_{global} = \frac{1}{N(N-1)} \sum_{i \neq j} \frac{1}{L_{i,j}}. \quad (5)$$

The small-world coefficient (σ) is defined as:

$$\sigma = \frac{C_{real} L_{random}}{L_{real} C_{random}}. \quad (6)$$

If $\sigma > 1$, the studied network has small-world characteristics.

2.6. Relief-F

Relief-F [24] represents Kononeill's expansion of relief in 1994, which can be used to address multi-category problems. When the Relief-F algorithm deals with multiple types of problems, it randomly takes a sample R from the training sample set each time, after which it finds the k nearest neighbor samples (near hits) of R from the sample set of the same type as R. Subsequently, it finds k nearest neighbor samples (near misses) in the sample set, and then updates the weight of each feature:

$$\delta^j = \sum_i -\mathrm{diff}(x_i^j, x_{i,nh}^j)^2 + \sum_{l \neq k} (p_l \times \mathrm{diff}(x_i^j, x_{i,l,nm}^j)^2) \quad (7)$$

where p_l is the proportion of class l samples in dataset D.

2.7. Statistical analysis

Independent (unpaired) sample t-tests [25] were used to compare the difference between the TE connection matrices of the three hand movements. Since multiple statistical tests have been performed on the same data set, here we used false discovery rate (FDR) [26] to perform multiple comparison correction, and then averaged the corrected FDR values as the p. The significance level of all statistical analyses is set to $p < 0.05$.

2.8. 5 × 2 cross-validation

Relevant or similar regression models tend to overfit the data, and the results often fail to be generalized to new data. Some brain behavior studies are not cross-verified, which makes it difficult to evaluate the universality of the results. Proper cross-validation is vital to ensure independence between feature selection and prediction/classification, thereby eliminating spurious effects and incorrect overall level inferences. Owing to our limited number of data sets, when using the cross-validation test estimation method, the training sets of different rounds overlap to a certain extent, resulting in an error rate that is not actually independent and leading to the overestimation of the probability of the hypothesis being true. To alleviate this problem, we used a '5 × 2 cross-validation'. Here, we use python to write a script to randomly divide all the data of each movement sample according to the ratio of the training set to the test set of 4:1, and then combine the data into a training set and a test set. And then perform training and testing, and perform five iterations to obtain an average accuracy.

3. Results

3.1. TE connection matrix

We analyzed the EEG and EMG data recorded from six participants during MF, OH, and WF movements. However, due to the interference of various factors in the collection process of the experiment, a total of 54 sets of MF, 52 sets of OH, and 47 sets of WF were collected. As shown in figure 4, the processed EEG and EMG data were filtered into four frequency bands (theta: 4–8 Hz, alpha: 8–13 Hz, beta1: 13–21 Hz, and beta2: 21–35 Hz). For each participant and experimental action, we calculated the TE connection matrix from cortex to cortex (EEG → EEG), cortex to muscle (EEG → EMG), muscle to cortex (EMG → EEG), and muscle to muscle (EMG → EMG) electrodes from the filtered time series. Finally, the TE connection matrix was averaged and summarized among the participants. For the theta and alpha frequency bands, the values of TE between the cortical electrode and the muscle electrode were very small, while the beta1 and beta2 frequency bands were the opposite (figures 5(a)–(c)), indicating that the beta wave is the main information carrier for all the participants to perform the three hand movements. We found that the mean values of the TE between EEG → EMG and EMG → EEG were close (figures 5(a)–(c)), indicating that the information transmission between the cortex and the muscles is bidirectional.

Second, we sought to better understand the TE connection matrix. For each participant and experimental action, we calculated the TE between each electrode of the cortex and the muscles. As shown in figure 6, the TE connection matrix of each participant's three hand movements in four frequency bands was displayed in the form of a heat map.

Comparing the heat map of the TE connection matrix of different hand movements of the same participant revealed that there are certain differences between them (figures 6(a)–(c)). We aimed to test whether the TE connection matrix could be used to recognize hand movements. We performed t-tests between the same actions and different actions on the TE connection matrix of 54 groups of MF movements, 52 groups of OH movements, and 47 groups of WF movements calculated for all participants (table 1). We determined that there is a significant difference ($p < 0.05$) in the TE connection matrix between the same action in the theta and alpha

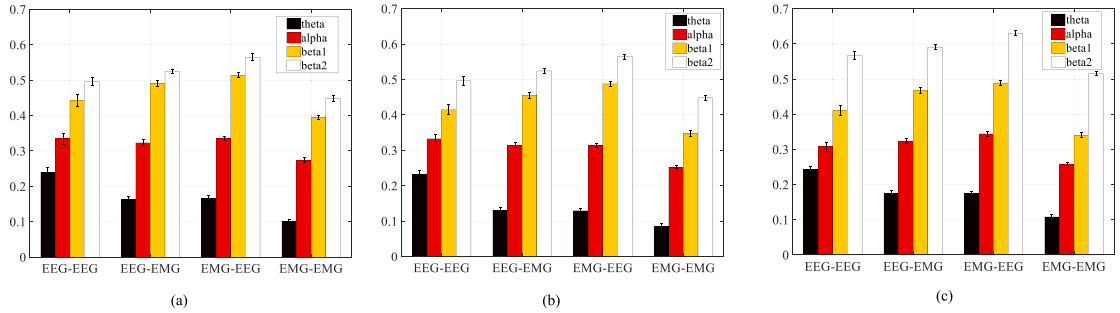

Figure 5. Mean values and standard deviation of different TE connection matrices (EEG → EEG, EEG → EMG, EMG → EEG, and EMG → EMG) in four frequency bands (theta, alpha, beta1, and beta2) for three actions: (a) MF, (b) OH, and (c) WF.

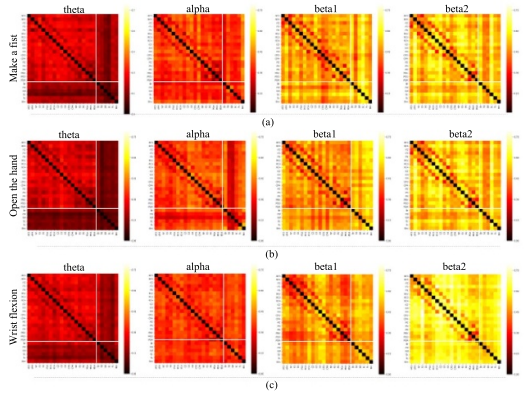

Figure 6. Heat map of TE connection matrix: (a) MF, (b) OH, and (c) WF.

bands. This indicates that the TE connection matrix of theta and alpha bands cannot be used as the classification feature for the three hand movements, which is possibly related to the fact that the theta and alpha waves are not the main information carriers involved when participants perform the three hand movements. However, for the beta1 and beta2 bands, as expected, there were significant differences ($p < 0.05$) between different actions, but there were no significant differences ($p > 0.05$) between the same actions. This result revealed that the TE connection matrix of the beta1 and beta2 bands can be accurately used to classify these three hand movements.

3.2. Network characteristics

In this study, we selected the edges of the top 15% connection strength as the threshold (T) for binarization in all frequency bands, which is the preference of previous researchers [27, 28]. Such a threshold selection could ensure that the CMFN is neither a very sparse nor dense graph. We calculated the C, L, and E_{global} using Matlab's Brain Connectivity Toolbox [29]. In figure 7, we show the mean value of C and E_{global} of the TE connection matrix of the three hand movements at 15% network density. We observed that the mean value of C in the beta1 and beta2 bands is larger, while they are generally smaller in the theta and alpha bands (figure 7(a)), indicating that the electrical activity in the participants' brains during hand movement mainly consists of beta waves. It is worth noting that in the beta1 and beta2 frequency bands, the mean value of the C is largest for WF, followed by the MF movement, whereas the OH movement is the smallest, which may be indicative of the degree of cortical and muscular involvement associated with the different movements. We compared the mean of the E_{global} of the three hand movements (figure 7(b)). We observed that the mean E_{global} of the three hand movements are not significantly different but are more similar in the beta2 band. This suggests that there may be more components of the beta2 wave when the participants perform hand movements. Moreover, it indicates that the overall information transmission efficiency of the cortex and the muscles during different movements is similar.

Many scholars have demonstrated that the functional network of the brain has small-world attributes [30–32]. Here, we sought to ascertain whether the CMFN also has small-world attributes. First, we constructed 50 random networks with the same number of nodes, and calculated the average of C and L. In figure 8, we show the mean values of σ for the three actions in the four bands. It can be clearly seen that both the beta1 and beta2 frequency bands have small-world attributes ($\sigma > 1$), whereas the theta and alpha frequency bands have the opposite attributes. At the same time, we also noticed that in the beta1 and beta2 bands, the WF movement displayed the largest σ, followed by the MF movement and that of the OH movement being the smallest. This suggests that σ may be related to the difficulty of the action. It is worth noting that the σ of the beta2 band in the three actions is slightly higher than that of the beta1 band. This phenomenon was also found when calculating the mean value (figures 5(a)–(c) and C (figure 7(a)) of the TE connection matrix. This indicated that the participants had greater beta2 involvement in the electrical activity in their brains when performing the three hand movements. Therefore, we focused on the beta2 frequency band for further investigation.

Table 1. *T*-test (95% confidence interval) between and within MF, OH, and WF groups.

	Theta	Alpha	Beta1	Beta2
Within MF groups	$p = 0.031^*$	$p = 0.357$	$p = 0.330$	$p = 0.542$
Within OH groups	$p = 0.045^*$	$p = 0.034^*$	$p = 0.253$	$p = 0.473$
Within WF groups	$p = 0.018^*$	$p = 0.043^*$	$p = 0.441$	$p = 0.492$
Between MF and OH groups	$p = 0.033^*$	$p < 0.01^*$	$p = 0.031^*$	$p = 0.036^*$
Between MF and WF groups	$p = 0.037^*$	$p = 0.017^*$	$p < 0.01^*$	$p < 0.01^*$
Between OH and WF groups	$p = 0.034^*$	$P = 0.021^*$	$p < 0.01^*$	$p < 0.014^*$

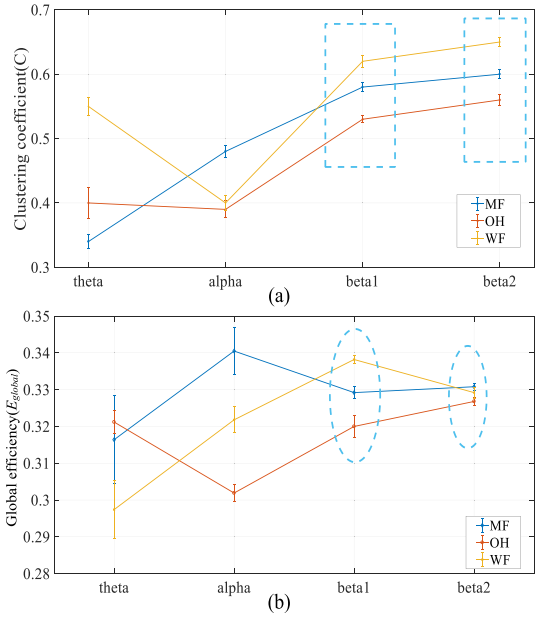

Figure 7. Network characteristics of the CMFN. (a) The mean and standard deviation of *C* of the CMFN of three hand movements. (b) The mean and standard deviation of E_{global} of CMFN for three hand movements.

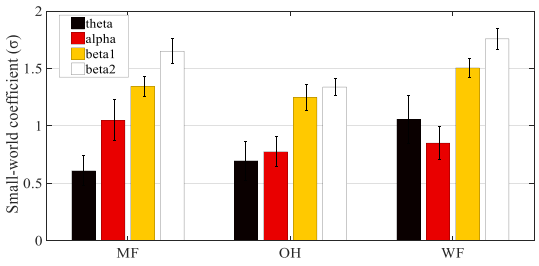

Figure 8. The mean and standard deviation of σ of the CMFN.

In order to better understand the CMFN, we superimposed and averaged the TE connection matrix of the beta2 band of each action, and then performed a threshold (*T*, the top 15% connection strength) binarization of the matrix. As shown in figure 9, a directed connection diagram of the three hand movements was generated. We found that in the directed connection diagram of these three actions, the most closely connected is the left motor area and its related muscles, which may indirectly indicate that the body's limb movement is mainly controlled by the

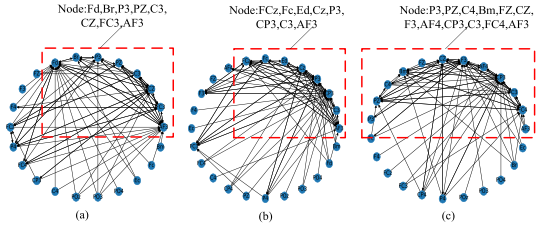

Figure 9. Directed connection diagram. (a) MF, (b) OH, and (c) WF.

contralateral movement area. By simple visual inspection, the directed connection graph of the three hand movements was found to be between the random network and the regular network, with the characteristics of a small-world network, as was also verified in the above calculations (figure 8).

3.3. Action recognition

In the experiment, we found that there are significant differences in the TE connection matrix of the three actions in the beta2 band (table 2). Therefore, the TE connection matrix was used as the classification basis for these three actions. First, using each directed edge of the TE connection matrix as a feature, there was a total of 600 ($25 \times (25 - 1)$) features. Second, we set the labels of the TE connection matrix of 54 groups of MF movements, 52 groups of OH movements, and 47 groups of WF movements to 1, 2, and 3, respectively. Finally, these labeled TE connection matrices were input into the Relief-F script written by Python to extract the top 20 features with the best classification effect (figure 10(b) and 20 features of extraction). In figure 10(a), we randomly extracted three sets of TE connection matrices from each action, and demonstrated the feature value of each action. In this drawing, each point represents the TE value from one electrode to the other. This is shown in figure 9(c), which displays the extracted features in the human body model in the form of directed edges. We observed that the feature edges were mainly concentrated in the left cortical area and between the cortex and the muscles. This also indicates that the movement of the human body is related to the contralateral cortex area and its related muscles, and might also be used to explore the role of different areas of the CMFN. It is worth noting that most connected nodes are mainly concentrated in the left frontal area (AF3,

Table 2. Results of the training classification of three movements.

	20 features	15 features	10 features	5 features
SVM	84.17%	75.49%	69.63%	55.75%
LR	83.03%	73.78%	67.12%	54.93%

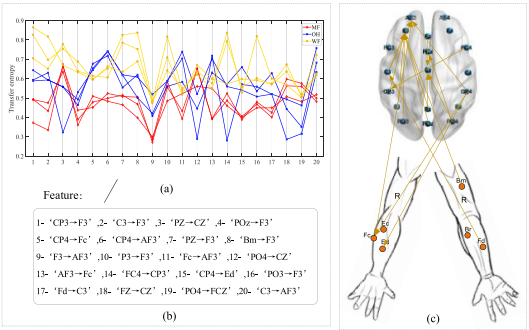

Figure 10. Twenty feature edges extracted from the TE connection matrix of three hand movements with Relief-F. (a) The corresponding value of the extracted feature in the TE connection matrix. (b) Twenty extraction features. (c) The specific area corresponding to the extracted feature edge in the human body model.

F3), and that the frontal lobe area may be expected to play a significant role in human limb movement, the energy in the averaged topographical map of the brain is also mainly concentrated in this area (figure 4(a)). We have observed that not all muscles are connected to the cortex, only Fc, Ed, Fd, and Bm are connected, and Fc, Ed, and Fd are directly related to the three actions [33], This is also reflected in the time domain diagram of the action (figure 4(b)). This shows that the CMFN we have established can be applied to study human body movements.

To classify the three hand movements, first, extract the first 20 features, the first 15 features, the first 10 features and the edges of the first 5 features corresponding to each TE connection matrix to construct a new data sample with labels. Second, we used Python's sklearn [34] package to build the SVM and LR trainer, and finally, we performed a 5 × 2 cross-validation on the data samples, obtaining the average accuracy of the training model. Table 2 shows the average accuracy of the recognition of these three actions by the two models. It can be clearly seen that when the first 20 features are used for classification, the accuracy of SVM reaches 84%. Furthermore, when the first 15 features are used, the accuracy can reach 75%, and when only the first 5 features are used, the accuracy is close to 55%. This indicates that the TE connection matrix can be used for hand movement classification and can achieve a high classification accuracy.

4. Discussion

In this study, we proposed a new functional network using EEG and EMG data to construct a CMFN. This network helped to analyze the relationship between the cortex and the muscles. We constructed a CMFN and analyzed the MF, OH, and WF movements of six participants. James *et al* [35] indicated that all subjects showed significant continuity (0.086–0.599) between the MEG and muscles in the 15–30 Hz range when controlling the robot lever. In our research, we confirmed that the TE connection matrix of hand movements had the strongest causal relationship in the beta1 and beta2 band (13–35 Hz), and that the causal relationship was slightly greater in the beta2 band than in the beta1 frequency band (figures 5(a)–(c)). This result indicates that beta waves can be the carrier of motor cortex information, which is consistent with Takahashi's results [36]. However, the mean values of the TE connection matrix of EEG → EMG and EMG → EEG on the theta frequency band remain very small (figures 5(a)–(c)), which suggests that theta waves are not a medium for information transmission between the cortex and the muscles; the lack of exercise-related components in the theta wave in EMG signals may also be involved.

When we analyzed the complex network characteristics of the CMFN, we found that they have small-world attributes in the beta1 and beta2 frequency bands. Interestingly, in the beta1 and beta2 frequency bands, the σ (figure 8) and C (figure 7(a)) of the WF movement were the largest, followed by those of the MF with those of the OH being the smallest. Danielle Smith's research on small world networks shows that there is a close relationship between small world topology and dynamic complexity [37]. Small world networks have high global efficiency and high local efficiency or low-cost fault tolerance. The clustering coefficient can be considered a measure of the local efficiency of information transmission [23]. These indicate that with higher σ and C, the global and local efficiency of information transfer between nodes are relatively high. Here we assume that the reaction time of each participant has a negligible impact on the experiment, so in the same time, the more complex the completed action, the higher the efficiency of information transmission. These results indicate that the characteristics of the complex network of the CMFN are related to the complexity of the hand movements. WF movements have a relatively high complexity, requiring a greater degree of cooperation between the cortex and the muscles, while OH movements, in contrast, have relatively low complexity.

In our research, we used the TE connection matrix between the cortex and the muscles of the beta2 frequency band to recognize the hand movements. Previous studies mainly focused on the features of the original information. Shime *et al* [38] achieved an accuracy of 67% when classifying three different stretching movements of the same limb by decoding EEG. Avik *et al* [39] achieved an accuracy of 83.33% when classifying six different grasping actions by extracting important features from the original

EMG signal. Paulo *et al* [40] used an artificial neural network to classify hand movements and gestures using EMG from the two forearm muscles. The accuracy rate reached over 85%. Although these methods can achieve high recognition accuracy even higher than ours, they only reflect the characteristics of the signal and cannot reflect the coupling between the cortex and the muscles. Frederic *et al* [41] proposed a real-time gesture recognition system based on surface EMG signals. Five gesture sets supported by Myo armbands achieved an overall accuracy of 95%. They extracted ten equally-weighted features from both the time and the frequency domain (through a fast Fourier Transformation). Although our recognition results rely on EEG and EMG information intercepted at a fixed time, our research focus is different from Frederic *et al*. In this paper, we mainly used action recognition to verify the reliability of the difference between the cortical and muscle coupling between different hand movements extracted. This study aimed to link the CMFN with the actual movements of the individual, analyze the coupling between the cortex and the muscles during different hand movements, and perform movement recognition. When performing the right-hand stretch, the inferior frontal cortex and left primary motor area are activated [42]. In our research, we also found that the differences between participants in different hand movements were mainly concentrated in the left frontal area (AF3, F3), left motor cortex (C3), occipital lobe (PO4), and their related muscles (figure 10). Participants mainly used the instructions on the screen to perform corresponding actions during the experiment, which led to different visual stimuli, and may account for the PO4 nodes being found to be connected to many feature edges. The participants also may not have been very uniform when performing the hand movements in the experiment, so they also moved their elbows. This may be why Bm is also connected to the characteristic edge. These results all indicate that the CMFN we have established in the beta2 band can be effectively used to assess the coupling between the cortex and muscles. Future research should focus on stroke patients to analyze the patient's diseased areas.

This experiment was successful. However, due to the limited number of participants, the results need to be confirmed by future studies involving larger cohorts.

5. Conclusion

This study introduces a new functional network called the CMFN. We applied TE to establish the connection matrix between the cortex and the muscles and explore the coupling between the cortex and the muscles. The results demonstrated the successful application of the developed CMFN to analyze the transmission of information between the cortex and the muscles. Additionally, it can also be applied for gesture recognition, thus providing more insights regarding the transmission of information between the cortex and the muscles. Future research should continue to explore cortico-muscular coupling to provide a deeper understanding of the relationship between the cortex and the muscles. In the future, this information can potentially be applied for treating stroke patients.

Data availability statement

The data generated and/or analyzed during the current study are not publicly available for legal/ethical reasons but are available from the corresponding author on reasonable request.

Acknowledgments

This work was supported by the National Natural Science Foundation of China (Nos. 61971169, 62061044 and 60903084), and Zhejiang Provincial Key Research and Development Program of China (No. 2021C03031).

ORCID iDs

Xugang Xi https://orcid.org/0000-0002-9213-6313
Yun-Bo Zhao https://orcid.org/0000-0002-3684-5297

References

[1] Mima T and Hallett M 1999 Electroencephalographic analysis of cortico-muscular coherence: reference effect, volume conduction and generator mechanism *Clin. Neurophysiol.* **110** 1892–9
[2] Krauth R *et al* 2019 Cortico-muscular coherence is reduced acutely post-stroke and increases bilaterally during motor recovery: a pilot study *Front. Neurol.* **10** 126
[3] Artoni F, Fanciullacci C, Bertolucci F, Panarese A, Makeig S, Micera S and Chisari C 2017 Unidirectional brain to muscle connectivity reveals motor cortex control of leg muscles during stereotyped walking *Neuroimage* **159** 403–16
[4] Lai M-I, Pan L-L, Tsai M-W, Shih Y-F, Wei S-H and Chou L-W 2016 Investigating the effects of peripheral electrical stimulation on corticomuscular functional connectivity stroke survivors *Top. Stroke Rehabil.* **23** 154–62
[5] Betzel R F, Medaglia J D, Kahn A E, Soffer J, Schonhaut D R and Bassett D S 2019 Structural, geometric and genetic factors predict interregional brain connectivity patterns probed by electrocorticography *Nat. Biomed. Eng.* **3** 902–16
[6] Busonera G, Cogoni M, Puligheddu M, Ferri R, Milioli G, Parrino L, Marrosu F and Zanetti G 2018 EEG spectral coherence analysis in nocturnal epilepsy *IEEE Trans. Biomed. Eng.* **65** 2713–9
[7] Nimmy J T, Subha D and Menon R N (eds) 2019 Mutual information analysis on MCI-AD EEG signal during resting and task conditions *TENCON 2019-2019 IEEE Region 10 Conf. (TENCON)* (IEEE) (https://doi.org/10.1109/TENCON.2019.8929242)
[8] Benzy V and Vinod A (eds) 2019 Classification of motor imagery hand movement directions from EEG extracted phase locking value features for brain computer interfaces

TENCON 2019-2019 IEEE Region 10 Conf. (TENCON) (IEEE) (https://doi.org/10.1109/TENCON.2019.8929678)
[9] Omidvarnia A H, Azemi G, Boashash B, O'Toole J M, Colditz P and Vanhatalo S (eds) 2012 Orthogonalized partial directed coherence for functional connectivity analysis of newborn EEG *Int. Conf. on Neural Information Processing* (Springer)
[10] Li P, Huang X, Zhu X, Liu H, Zhou W, Yao D and Xu P 2018 LP ($p \leqslant 1$) norm partial directed coherence for directed network analysis of scalp EEGs *Brain Topogr.* **31** 738–52
[11] Vicente R, Wibral M, Lindner M and Pipa G 2011 Transfer entropy—a model-free measure of effective connectivity for the neurosciences *J. Comput. Neurosci.* **30** 45–67
[12] Shovon M H I, Nandagopal N, Vijayalakshmi R, Du J T and Cocks B 2017 Directed connectivity analysis of functional brain networks during cognitive activity using transfer entropy *Neural Process. Lett.* **45** 807–24
[13] Baars B J and Gage N M 2010 *Cognition, Brain, and Consciousness: Introduction to Cognitive Neuroscience* (New York: Academic)
[14] Papo D, Buldú J M, Boccaletti S and Bullmore E T 2014 *Complex Network Theory and the Brain* (Westminster, London: The Royal Society) (https://doi.org/10.1098/rstb.2013.0520)
[15] John M, Ikuta T and Ferbinteanu J 2017 Graph analysis of structural brain networks in Alzheimer's disease: beyond small world properties *Brain Struct. Funct.* **222** 923–42
[16] Li X *et al* 2017 A motion-classification strategy based on sEMG–EEG signal combination for upper-limb amputees *J. Neuroeng. Rehabil.* **14** 2
[17] Delorme A and Makeig S 2004 EEGLAB: an open source toolbox for analysis of single-trial EEG dynamics including independent component analysis *J. Neurosci. Methods* **134** 9–21
[18] Gómez-Herrero G *et al* (eds) 2006 Automatic removal of ocular artifacts in the EEG without an EOG reference channel *Proc. 7th Nordic Signal Processing Symp.-NORSIG 2006* (IEEE)
[19] Luck S J 2014 *An Introduction to the Event-Related Potential Technique* (Cambridge, MA: MIT Press)
[20] Vázquez R R *et al* 2012 Blind source separation, wavelet denoising and discriminant analysis for EEG artefacts and noise cancelling *Biomed. Signal Process. Control* **7** 389–400
[21] Daubechies I 1990 The wavelet transform, time-frequency localization and signal analysis *Int. J. Remote Sens.* **36** 961–1005
[22] Huang C-S, Pal N R, Chuang C-H and Lin C-T 2015 Identifying changes in EEG information transfer during drowsy driving by transfer entropy *Front. Hum. Neurosci.* **9** 570
[23] Bullmore E and Sporns O 2009 Complex brain networks: graph theoretical analysis of structural and functional systems *Nat. Rev. Neurosci.* **10** 186–98
[24] Kononenko I, Šimec E and Robnik-Šikonja M 1997 Overcoming the myopia of inductive learning algorithms with RELIEFF *Appl. Intell.* **7** 39–55
[25] Schober P and Vetter T R 2019 Two-sample unpaired *t*-tests in medical research *Anesth. Analg.* **129** 911
[26] Benjamini Y and Yekutieli D 2001 The control of the false discovery rate in multiple testing under dependency *Ann. Stat.* **29** 1165–88
[27] Redcay E, Moran J M, Mavros P L, Tager-Flusberg H, Gabrieli J D and Whitfield-Gabrieli S 2013 Intrinsic functional network organization in high-functioning adolescents with autism spectrum disorder *Front. Hum. Neurosci.* **7** 573
[28] Reineberg A E and Banich M T 2016 Functional connectivity at rest is sensitive to individual differences in executive function: a network analysis *Hum. Brain Mapp.* **37** 2959–75
[29] Whitfield-Gabrieli S and Nieto-Castanon A 2012 Conn: a functional connectivity toolbox for correlated and anticorrelated brain networks *Brain Connect.* **2** 125–41
[30] Wang J *et al* 2009 Parcellation-dependent small-world brain functional networks: a resting-state fMRI study *Hum. Brain Mapp.* **30** 1511–23
[31] Sporns O and Honey C J 2006 Small worlds inside big brains *Proc. Natl Acad. Sci.* **103** 19219–20
[32] Sporns O and Zwi J D 2004 The small world of the cerebral cortex *Neuroinformatics* **2** 145–62
[33] Martini F *et al* 2006 *Human Anatomy* (San Francisco, CA: Pearson/Benjamin Cummings)
[34] Pedregosa F *et al* 2011 Scikit-learn: machine learning in Python *J. Mach. Learn. Res.* **12** 2825–30
[35] Kilner J M, Baker S N, Salenius S, Hari R and Lemon R N 2000 Human cortical muscle coherence is directly related to specific motor parameters *J. Neurosci.* **20** 8838–45
[36] Takahashi K, Saleh M, Penn R D and Hatsopoulos N 2011 Propagating waves in human motor cortex *Front. Hum. Neurosci.* **5** 40
[37] Bassett D S and Bullmore E 2006 Small-world brain networks *Neuroscientist* **12** 512–23
[38] Shiman F, López-Larraz E, Sarasola-Sanz A, Irastorza-Landa N, Spüler M, Birbaumer N and Ramos-Murguialday A 2017 Classification of different reaching movements from the same limb using EEG *J. Neural Eng.* **14** 046018
[39] Bhattacharya A, Sarkar A and Basak P (eds) 2017 Time domain multi-feature extraction and classification of human hand movements using surface EMG *2017 4th Int. Conf. on Advanced Computing and Communication Systems (ICACCS)* (IEEE)
[40] Pl V, Vs F, Lm L, Gl O, Oliveira G C and Varoto R ed *et al* 2019 An artificial neural network for hand movement classification using surface electromyography *Biosignals* 185–92
[41] Kerber F, Puhl M and Krüger A 2017 User-independent real-time hand gesture recognition based on surface electromyography *Proc. 19th Int. Conf. on Human–Computer Interaction with Mobile Devices and Services* pp 1–7
[42] Liu Z and Luo Z (eds) 2008 Hand motion pattern classifier based on EMG using wavelet packet transform and LVQ neural networks *2008 IEEE Int. Symp. on IT in Medicine and Education* (IEEE) (https://doi.org/10.1109/ITME.2008.4743817)